Bifurcation routes in a laser with injected signal

Yan Gu,* Donna K. Bandy, Jian-Min Yuan, and Lorenzo M. Narducci
Physics Department, Drexel University, Philadelphia, Pennsylvania 19104
(Received 29 May 1984)

With the help of time-dependent solutions, their power spectra, Poincaré maps, and the complete set of Lyapunov exponents, we have carried out a detailed investigation of the bifurcation routes of three attractors in a single-mode model of a laser with injected signal. In addition to a sequence of ordinary period-doubling bifurcations leading to chaos, we have observed subcritical and supercritical Hopf bifurcations of limit cycles. We have also observed the sudden disappearance of trajectories due to the coalescence of a pair of stable and unstable tori and the possible collision of a limit cycle with an unstable torus.

Lasers and other coherent optical systems have long been known to undergo stability changes under appropriate conditions. A single-mode, homogeneously broadened, free-running laser, for example, is believed to develop output pulsations if the cavity linewidth and the unsaturated gain are sufficiently large.[1] This prediction has resisted experimental verification, but numerous instances of unstable behavior have been recorded for lasers with inhomogeneously broadened gain profiles.[2] Instabilities in bistable optical systems have also been investigated extensively[3] and the occurrence of self-pulsing is actively sought out experimentally in a ring-cavity system containing two-level atoms.[4]

The active counterpart of a bistable system is the so-called laser with injected signal, an ordinary laser operating above threshold and driven by a cw external field.[5] Theoretical studies of this system[6] have revealed the possibility of interesting scenarios that include a variety of pulsing modes of operation, including chaos.

The purpose of this paper is to summarize the results of an in-depth analysis of the bifurcation routes of a specific model of laser with injected signal using the combined diagnostic power of time-dependent solutions, power spectral calculations, Poincaré sections of surfaces, and Lyapunov exponents. We wish to provide not only a clarification of several open questions from a previous publication[6(b)] but also to demonstrate, with a specific nontrivial example, the value of these combined techniques for the analysis of complicated bifurcation patterns.

The system under study consists of a single-mode ring cavity containing a collection of homogeneously broadened two-level atoms. The atoms and the cavity are tuned to one another at a frequency $\omega_A=\omega_C$ and, in the absence of any external signal, produce a stable laser output with a carrier frequency ω_A. By injecting into the cavity a cw beam at frequency $\omega_0\neq\omega_A$, the potential for competition is established between the driving field and the laser oscillator. At low-signal levels the output of the system displays a beat pattern at frequency $|\omega_A-\omega_0|$ due to the mixing of the two fields, with the laser acting as a local oscillator. At very high external signal levels the laser is predicted to lock stably to the injected field and to produce a constant output intensity with a carrier frequency ω_0 (injection locking). Somewhere between these two limits complicated nonlinear phenomena emerge, as reported in Refs. 6(a) and 6(b).

The model is described by the usual single-mode Maxwell-Bloch equations

$$\frac{dx}{d\tau}=-\tilde{\kappa}(i\theta x+x-y+2Cp)\ , \tag{1a}$$

$$\frac{dp}{d\tau}=xD-(1+i\tilde{\Delta})p\ , \tag{1b}$$

$$\frac{dD}{d\tau}=-\tilde{\gamma}[\tfrac{1}{2}(xp^*+x^*p)+D+1]\ , \tag{1c}$$

where y and x are proportional to the incident and emitted field amplitudes (y is real and positive, for definiteness; x is complex) and p and D are the normalized complex polarization and population difference, respectively. The control parameters C, θ, $\tilde{\Delta}$, $\tilde{\kappa}$, and $\tilde{\gamma}$ represent the small-signal atomic gain, the cavity mistuning $[(\omega_C-\omega_0/\kappa]$, the atomic detuning $[(\omega_A-\omega_0)/\gamma_\perp]$, and the scaled cavity $(\kappa/\gamma_\perp)$ and population $(\gamma_\parallel/\gamma_\perp)$ relaxation rates. The time τ is measured in units of the polarization relaxation time, $\gamma_\perp^{-1}$.

With reference to the state equation $|x|=|x|(y)$ shown in Fig. 1, it will be useful to summarize the main results of an earlier scan[6(a),6(b)] in which the amplitude of the injected field was varied from 0 to about 20. For each value of y, we monitored the time evolution of the output intensity by solving Eqs. (1a)—(1c), with the system initially in the stationary state defined by the final configu-

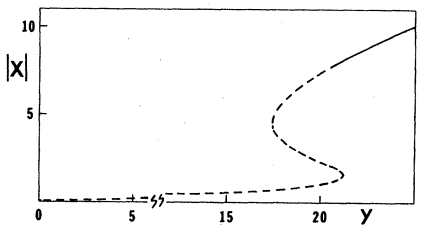

FIG. 1. State equation for a laser with injected signal corresponding to $C=20$, $\Delta=1$, $\theta=2$, $\tilde{\kappa}=0.5$, and $\tilde{\gamma}=0.05$. The dashed segment is a locus of unstable stationary states.

ration of the previous run (adiabatic scan). For $y \lesssim 6$ the output intensity was observed to undergo oscillations with a pulsing frequency $\tilde{\omega}_p \simeq \tilde{\Delta} = (\omega_A - \omega_0)/\gamma_\perp$. In the range $6 \lesssim y \lesssim 11$ the oscillations developed progressively larger distortion, while the pulsing frequency $\tilde{\omega}_p$ decreased monotonically from unity (the chosen value of $\tilde{\Delta}$) to approximately 0.8 [for further details of this aspect of our study, see Ref. 6(b)]. In this range of values of the driving field, we gained our first evidence of the existence of competing basins of attraction. In fact, by injecting *different* initial perturbations into the starting state of the system, we obtained quite different looking long-term oscillatory patterns. Beyond $y \gtrsim 11$ chaos set in, followed by an easily recognizable sequence of inverse period-doubling bifurcations, which eventually terminated at the injection locking threshold (a standard Hopf bifurcation point, if one varies y from higher to lower values).

Due to the complexity of the bifurcation sequences in the range $y \lesssim 13$, it became necessary to discriminate more closely among solutions that evolve under the action of coexisting basins of attraction. This was accomplished by calculating the power spectra of temporal solutions in the range $y \lesssim 13$. In Fig. 2 we show the dependence of the frequency of the fundamental spectral component on the control parameter y. As alluded to by the quite different character of the time records, the fundamental frequencies $\tilde{\Omega}_0$ of the power spectra confirm that distinct domains of attraction do coexist in the range $6 \lesssim y \lesssim 11$.

As a further refinement we have calculated all five Lyapunov exponents for Eqs. (1) and monitored at the same time the Poincaré sections of the trajectories. Before we enter into the details of these latest findings, it may be useful to provide a brief summary of the information that one can gather from the calculation of the Lyapunov exponents[7] (some pertinent, more technical details are given in the Appendix). Given a set of autonomous (usually nonlinear) differential equations of the type

$$\dot{x}_i = F_i(x_1, x_2, \ldots, x_N), \quad i = 1,2,\ldots,N \tag{2}$$

standard integration routines can produce the trajectory of a representative point $P \equiv (x_1, x_2, \ldots, x_N)$ in phase space. To test whether the trajectory is stable or not, one may select a point in the vicinity of the trajectory and follow its evolution according to the linearized equations of motion. If δx_i represents the initial deviation away from the selected value $x_i(t)$, and if $\vec{\mathrm{W}}$ denotes a vector whose components are proportional to the N-tuple $\{\delta x_i\}$, the linearized evolution of $\vec{\mathrm{W}}$ is described by

$$\dot{\vec{\mathrm{W}}} = \hat{J}\vec{\mathrm{W}} , \tag{3}$$

where $\hat{J}$ is the Jacobian matrix with elements

$$J_{ij} = \frac{\partial F_i(\vec{x})}{\partial x_j} . \tag{4}$$

One is interested in the rate of change of the length of $\vec{\mathrm{W}}$. If $\hat{J}$ is a constant matrix, the Lyapunov exponents are the real parts of the eigenvalues of $\hat{J}$ [this only happens if the selected starting point lies in the neighborhood of a steady state of the system (2)]. In general, of course, $\hat{J}$ will be time dependent because the point P itself is moving in phase space. Let

$$\vec{\mathrm{W}}(t) = T\left[\exp \int_{t_0}^{t} \hat{J}(t')dt'\right]\vec{\mathrm{W}}(t_0) \equiv \hat{U}(t,t_0)\vec{\mathrm{W}}(t_0) \tag{5}$$

be the solution of Eq. (3), where T is the usual time-ordering operator. The matrix $\hat{U}(t,t_0)$ can be written as the product $\hat{O}(t,t_0)\hat{S}(t,t_0)$ of an orthogonal ($\hat{O}$) and a non-negative ($\hat{S}$) matrix whose action is to induce rotations and dilatations of the N-dimensional vector space. Denote with λ_i the eigenvalues of $\hat{S}(t,t_0)$; then, by definition, the ith Lyapunov exponent is given by

$$E_i^L \equiv \lim_{t\to\infty} \frac{1}{t - t_0} \ln\lambda_i(t,t_0) . \tag{6}$$

In the following we adopt the common ordering convention $E_1^L \geq E_2^L \geq \cdots \geq E_N^L$.

Some of the main properties of the Lyapunov exponents that make them a very useful tool for stability considerations are listed below.

(1) Different types of attractors exhibit different Lyapunov exponents' characteristics. For autonomous dynamical systems, this characterization is summarized in Table I.

(2) The nature of certain bifurcations of a limit cycle can be uncovered by tracing the dependence of the Lyapunov exponents on the control parameters. Thus:

(i) If the limit cycle undergoes a period-doubling or symmetry-breaking bifurcation (the original basin of attraction splits into two domains of attraction), E_2^L will show a maximum of zero at the bifurcation point.

(ii) If the limit cycle undergoes a tangent bifurcation,

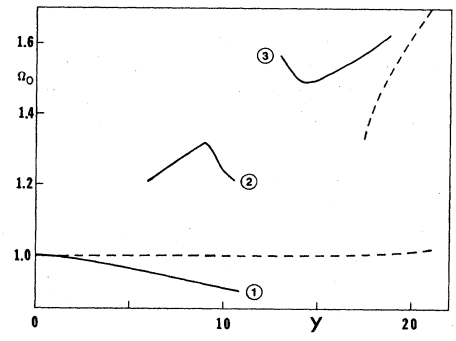

FIG. 2. The behavior of the fundamental-frequency component Ω_0 of the power spectrum. Lines 1 and 2 correspond to the fundamental frequencies of solutions that evolve under the influence of distinct domains of attraction. For a certain range of values of y, these domains coexist. Line 3 traces the behavior of the fundamental frequency through a sequence of period-doubling bifurcations. The dashed lines correspond to the imaginary part of the unstable eigenvalue of the linearized equations.

TABLE I. Attractors and their Lyapunov exponent characteristics.

Type of attractor	Lyapunov exponent characteristics
Steady state	$E_1^L < 0$
Limit cycle	$E_1^L = 0, \quad E_2^L < 0$
m-dimensional torus	$E_1^L = E_2^L = \cdots E_m^L = 0, \quad E_{m+1}^L < 0$
Chaos	$E_1^L > 0$

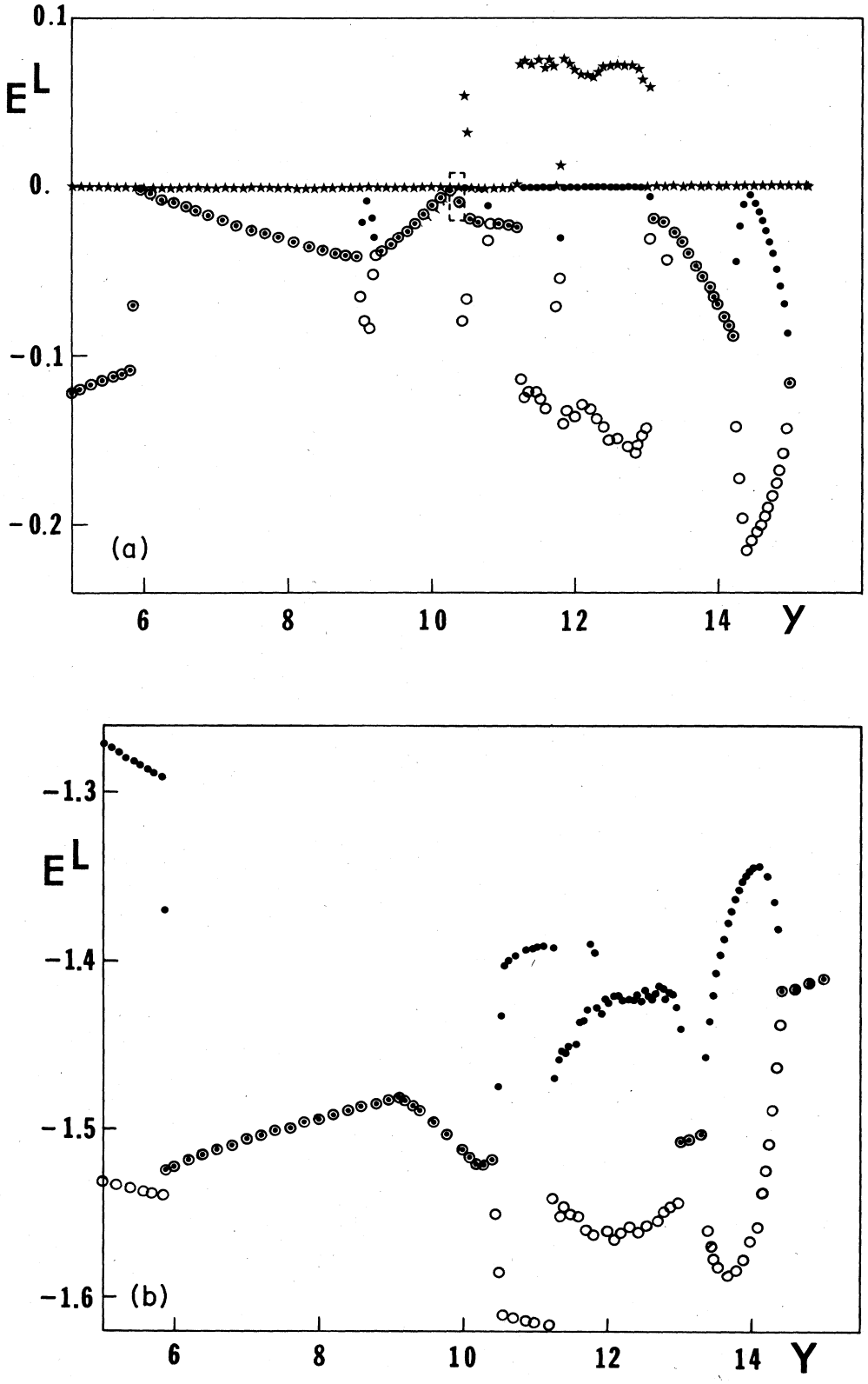

FIG. 3. (a) Behavior of the first three Lyapunov exponents as functions of the driving field y. The stars denote E_1^L, the dots denote E_2^L, and the open circles denote E_3^L. (b) Behavior of the Lyapunov exponents E_4^L (dots) and E_5^L (open circles) as functions of the driving field y. (c) Enlarged view of the first three Lyapunov exponents in the dashed box of (a).

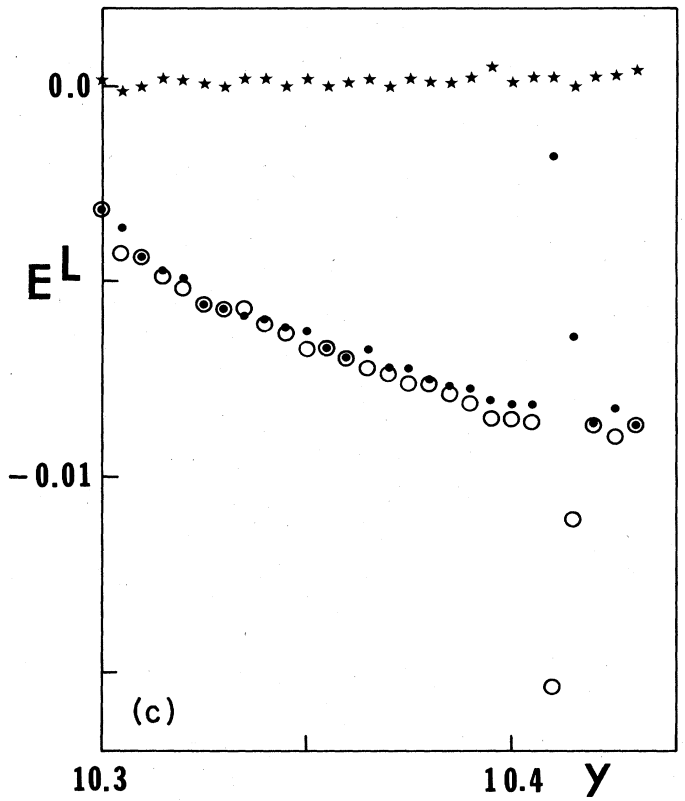

FIG. 3. (*Continued*).

E_2^L will first increase up to a value of zero; then, above the bifurcation point, either E_1^L becomes positive (while E_2^L remains zero) or E_2^L undergoes a sudden jump. The latter case is indicative that the trajectory has jumped into another coexisting attractor.

(iii) If the limit cycle undergoes a Hopf bifurcation as the control parameters are varied, one will have $E_2^L = E_3^L$ over a finite range of the parameters before the bifurcation point; this is a consequence of the fact that the corresponding eigenvalues of $\hat{U}(t,t_0)$ in Eq. (6) form a complex-conjugate pair. The subcritical or supercritical nature of the Hopf bifurcation can be recognized by the behavior of E_2^L and E_3^L above the bifurcation point. Thus, if E_1^L and E_2^L remain zero while E_3^L becomes negative again, the bifurcation is supercritical; if E_1^L becomes positive or E_2^L and E_3^L undergo a sudden change, the bifurcation may be expected to be subcritical.

(iv) If the second Lyapunov exponent of a limit cycle shows a sudden change without first becoming equal to zero, this may be a symptom of a collision of the limit cycle with the boundary of its basin, followed by the sudden disappearance of the limit cycle.

By using the adiabatic scanning technique, we have calculated the five Lyapunov exponents of our system from $y=15$ to $y=5$ as shown in Fig. 3. On observing a sudden change in dynamical behavior, as indicated by the Lyapunov exponents and the phase portraits, we have always reversed the direction of variation of y and searched for the existence of hysteretic behavior. Following this procedure, we have produced a global view of the main dynamical features of our system as shown synthetically in Fig. 4, where the individual attractors are denoted by their Poincaré section labels.

Each of the three branches in Fig. 4 portrays the bifurcation scheme of an attractor. As hinted by the time-dependent solutions, and confirmed by the analysis of their power spectra, more than one attractor may exist for the same value of y. In fact, Fig. 4 shows a fairly large domain of coexistence of two attractors and even a narrow region where three distinct attractors coexist.

Branch I begins at $y=0$ and ends at $y=11.12$. The numerical calculation of the five Lyapunov exponents supports the following relation:

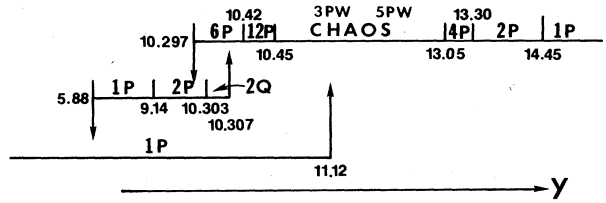

FIG. 4. Global behavior of the system in the range $0<y\lesssim 15$. 1P denotes a simple periodic solution, 2P is a doubly periodic solution (i.e., the spectrum contains a fundamental frequency ω and its subharmonic $\omega/2$), etc., 2Q denotes quasiperiodic motion with two incommensurate frequencies (two-dimensional torus), W denotes a window in chaos (thus, 3PW denotes a window with a triply periodic solution), and the values of y, e.g., $y=11.12$ at the end of domain I, denote the approximate thresholds.

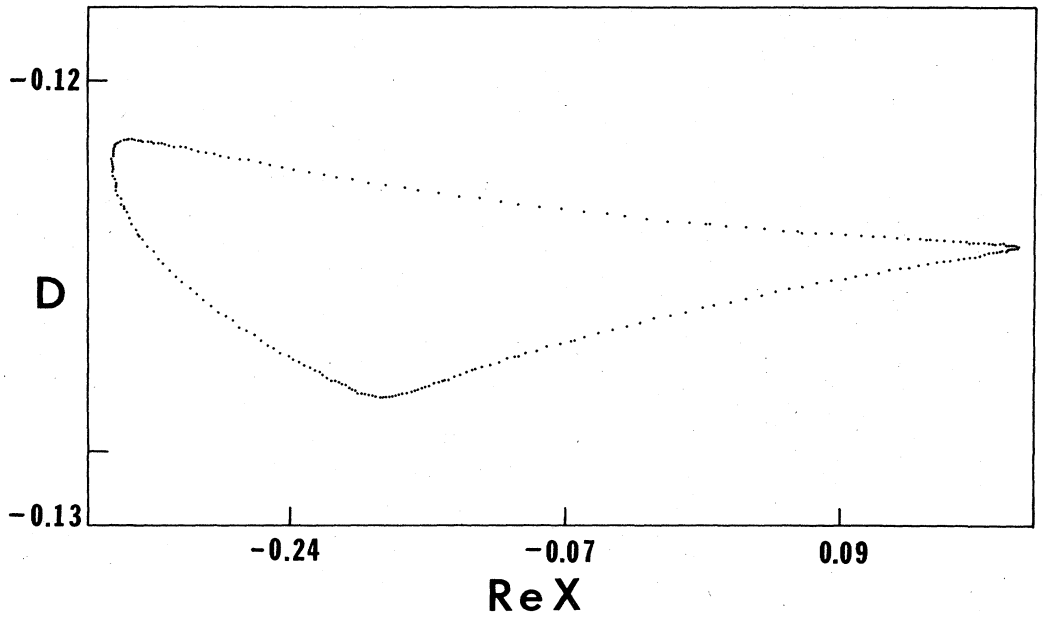

FIG. 5. Poincaré surface of section displaying an enlarged view of one-half of the 2Q torus for $y=10.307$, $\mathrm{Im}(x)=-6.0$.

$$0=E_1^L>E_2^L=E_3^L>E_4^L>E_5^L .$$

In particular, in the vicinity of $y=11.12$ (but for $y\lesssim 11.12$) we have

$$|E_1^L|\simeq|E_2^L|\simeq|E_3^L|<10^{-3} ,$$

$$E_4^L\simeq -1.460,\quad E_5^L\simeq -1.590 .$$

This indicates that a Hopf bifurcation occurs at $y=11.12$ because both E_2^L and E_3^L approach zero. No stable torus exists beyond this Hopf bifurcation; however, by selecting different initial points in the vicinity of the 1P limit cycle for $y\lesssim 11.12$, and by monitoring the transient evolution of the system in a Poincaré surface of section, we have identified the existence of an unstable torus which contracts into the limit cycle as y approaches the value 11.12 from below. On the basis of this evidence we conclude that the Hopf bifurcation at $y=11.12$ is of a subcritical type. Similar evidence supports the conclusion that a subcritical Hopf bifurcation also arises when y approaches the value 5.88 along branch II from above. This conclusion is also confirmed by the behavior of the Lyapunov exponents (Fig. 3).

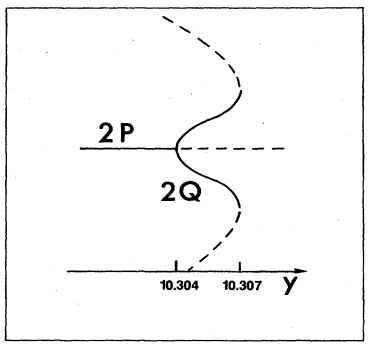

FIG. 6. Schematic representation of the supercritical bifurcation occurring at $y=10.307$ on branch II. The solid lines denote the stable 2P solutions and the 2Q torus, respectively. The dashed lines denote the unstable limit cycle and the unstable torus, respectively.

Another Hopf bifurcation occurs in branch II for $y\simeq 10.303$. Beyond this bifurcation point a stable torus (2Q) develops for which evidence, through the appearance of a second frequency, had been provided by the power spectra (Fig. 5). Hence, the bifurcation is supercritical as indicated schematically in Fig. 6. In addition, during a systematic search for the basin of attraction of the 2Q torus, we observed the existence of a second (unstable) torus surrounding the first. By increasing the value of y, it became apparent, from the behavior of the trajectories on the Poincaré surface of section, that the unstable torus converges to the stable one and eventually coalesces with it. This suggests the existence of a saddle-node-type bifurcation at $y\simeq 10.307$ (Fig. 6).

Branch III begins with a 6P limit cycle at $y=10.297$. The numerical results of the Lyapunov exponents show that in the neighborhood of and above $y=10.297$ we have

$$|E_1^L|<10^{-3},\quad E_2^L\simeq E_3^L\simeq -0.003 ,$$

$$E_4^L\simeq E_5^L\simeq -1.522 .$$

Because E_2^L remains negative when y approaches the value 10.297 from above, the sudden disappearance of the limit cycle can be explained only by the possible loss of stability of some points on the cycle itself (in contrast to the loss of stability of the entire trajectory in an ordinary bifurcation).

From Fig. 4, we observe that immediately after the disappearance of the 6P cycle, the basin of the original 6P attractor becomes the basin of the 2P attractor of branch

II. This suggests the reasonable assumption that the loss of stability of the 6P attractor is caused by its collision with the unstable torus of branch II whose presence was revealed by the bifurcation of the 2Q torus at $y=10.307$.

In conclusion, the combination of time-dependent studies, power spectra, Poincaré maps, and Lyapunov exponents have revealed progressively finer details of the very rich bifurcation structure of the single-mode model of a laser with injected signal. Further studies are in progress for different values of the gain and the detuning and mistuning parameters.

We are grateful to Professor N. B. Abraham for many useful discussions and comments. This research was partially supported by a grant from the Martin-Marietta Research Laboratories and by the U.S. Army Research Office under Contract No. DAAG29-82-K-0021. The support of the Ministry of Education of the People's Republic of China during the stay of Y.G. is gratefully acknowledged.

APPENDIX

The purpose of this appendix is to summarize a few technical details of the algorithm that was used in our computation of the Lyapunov exponents. This algorithm is based on the method developed by Benettin *et al.*[7]

We do not evaluate the Lyapunov exponents by calculating the eigenvalues λ_i $(i=1,2,\ldots,N)$ according to the definition (6). Instead, we choose arbitrary orthonormal sets $\{\vec{W}_j^0;\ j=1,\ldots,k\}$, $k\le N$ as initial vectors for the linearized differential equations (3) and calculate the exponential evolution rates of the volumes of the parallelepipeds generated by these sets. In fact, according to a theorem proved in Ref. 6(b), one has

$$\sum_{j=1}^{k} E_j^L=\lim_{t\to\infty}\left[\frac{1}{t}\ln||\vec{W}_1(t)\wedge\cdots\wedge\vec{W}_k(t)||\right], \quad k=1,\ldots,N \tag{A1}$$

where $\vec{W}_j(t)=\hat{U}(t,0)\vec{W}_j^0$, $||\vec{W}_1\wedge\cdots\wedge\vec{W}_k||$ denotes the volume of the k-dimensional parallelepiped generated by $\vec{W}_1,\ldots,\vec{W}_k$, and $E_1^L\ge E_2^L\ge\cdots\ge E_k^L$ are the largest k Lyapunov exponents.

In the actual computation of the Lyapunov exponents, the exponential growth (or reduction) of the volume $||\vec{W}_1(t)\wedge\cdots\wedge\vec{W}_k(t)||$ may be the source of numerical difficulties which can be circumvented by the use of the Gram-Schmidt procedure to reorthonormalize the set $\{\vec{W}_j(t)\,|\,j=1,\ldots,N\}$ after a selected time interval τ. This is done as follows.

By standard integration routines, we first calculate the vectors

$$\vec{V}_j^1=\hat{U}(\tau,0)\vec{W}_j^0,\quad j=1,\ldots,N \tag{A2}$$

and orthonormalize them successively with the help of the recursive formulas

$$\vec{a}_j^1=\vec{v}_j^1-\sum_{l=1}^{j-1}(\vec{v}_l^1\cdot\vec{w}_l^1)\vec{w}_l^1,$$
$$\vec{w}_j^1=\vec{a}_j^1/\alpha_j^1,\quad \alpha_j^1=||\vec{a}_j^1||,\quad j=1,2,\ldots,N. \tag{A3}$$

The volume of the k-dimensional parallelepiped generated by $\{\vec{v}_j^1\,|\,j=1,\ldots,k\}$ can be expressed as

$$||\vec{v}_1^1\wedge\cdots\wedge\vec{v}_k^1||=\prod_{j=1}^{k}\alpha_j^1.$$

We repeat this procedure with $\{\vec{w}_j^m\,|\,j=1,\ldots,N\}$ as initial vectors at $t=m\tau$, $m=1,2,\ldots$ and thus calculate successively the set of numbers $\{\alpha_j^m\,|\,j=1,\ldots,N\}$.

Since, given any two linearly equivalent sets of vectors $\{\vec{a}_j\,|\,j=1,\ldots,k\}$ and $\{\vec{b}_j\,|\,j=1,\ldots,k\}$, the following relation holds:

$$\frac{||\hat{U}(t,t_0)\vec{a}_1\wedge\cdots\wedge\hat{U}(t,t_0)\vec{a}_k||}{||\vec{a}_1\wedge\cdots\wedge\vec{a}_k||}=\frac{||\hat{U}(t,t_0)\vec{b}_1\wedge\cdots\wedge\hat{U}(t,t_0)\vec{b}_k||}{||\vec{b}_1\wedge\cdots\wedge\vec{b}_k||},$$

one also has

$$\begin{aligned}\ln||\vec{w}_1(m\tau)\wedge\cdots\wedge\vec{w}_k(m\tau)||&=\sum_{l=1}^{m}\ln\frac{||\vec{w}_1(l\tau)\wedge\cdots\wedge\vec{w}_k(l\tau)||}{||\vec{w}_1((l-1)\tau)\wedge\cdots\wedge\vec{w}_k((l-1)\tau)||}\\&=\sum_{l=1}^{m}\ln\frac{||\hat{U}(l\tau,(l-1)\tau)\vec{w}_1^{l-1}\wedge\cdots\wedge\hat{U}(l\tau,(l-1)\tau)\vec{w}_k^{l-1}||}{||\vec{w}_1^{l-1}\wedge\cdots\wedge\vec{w}_k^{l-1}||}\\&=\sum_{j=1}^{k}\sum_{l=1}^{m}\ln\alpha_j^l.\end{aligned} \tag{A4}$$

On comparing Eqs. (A4) and (A1), one obtains

$$E_j^L=\lim_{m\to\infty}\left[\frac{1}{m\tau}\sum_{l=1}^{m}\ln\alpha_j^l\right],\quad j=1,2,\ldots,N. \tag{A5}$$

Our numerical integration was carried out by a double-precision fourth-order Runge-Kutta method with a typical integration step size of 0.02. The reorthonormalization interval was chosen as $\tau=1$ and the number m in Eq. (A5) usually larger than 10^4. Because our dynamical system is autonomous, the largest Lyapunov exponents for limit cycles must be equal to zero. We have used this property to test the accuracy of our numerical scheme and noted that with the exception of the domains in control parameter space where critical slowing down becomes significant, our calculated Lyapunov exponents can be expected to be accurate to within about 10^{-3}.

*Permanent address: Physics Department, Lanzhou University, Lanzhou, Gansu, People's Republic of China.

[1]H. Haken, Z. Phys. **190**, 327 (1966); H. Risken, C. Schmid, and W. Weidlich, *ibid.* **194**, 337 (1966); H. Risken and K. Nummedal, Phys. Lett. **26A**, 275 (1968); J. Appl. Phys. **39**, 4662 (1968).

[2]K. R. Manes and A. E. Siegman, Phys. Rev. A **4**, 373 (1971); L. W. Casperson and A. Yariv, IEEE J. Quantum Electron. **QE-8**, 69 (1972); L. W. Casperson, *ibid.* **QE-14**, 756 (1978); Phys. Rev. A **21**, 911 (1980); **23**, 248 (1981); J. Bentley and N. B. Abraham, Opt. Commun. **41**, 52 (1982); M. Maeda and N. B. Abraham, Phys. Rev. A **26**, 3395 (1982); R. S. Gioggia and N. B. Abraham, Phys. Rev. Lett. **51**, 650 (1983).

[3]The following two extensive reviews are scheduled to be published in the very near future: L. A. Lugiato, in *Progress in Optics, Vol. XXI,* edited by E. Wolf (North-Holland, Amsterdam, in press) and H. M. Gibbs and S. McCall, *Optical Bistability* (Academic, San Francisco, in press). Additional references of published works can be found in L. M. Narducci, D. K. Bandy, J. Y. Gao, and L. A. Lugiato, in *Synergetics From Microscopic to Macroscopic Order,* edited by E. Frehland (Springer, Berlin, 1984), p. 33, and in *Optical Bistability,* edited by C. M. Bowden, M. Ciftan, and H. Robl (Plenum, New York, 1981).

[4]A beautiful demonstration of bistable action in a ring cavity with two-level atoms is described in D. E. Grant and H. J. Kimble, Opt. Commun. **44**, 415 (1983). The same basic system is under investigation to verify the theoretical predictions concerning self-pulsing behavior [H. J. Kimble (private communication)].

[5]Consideration of an injected signal as a means of stabilizing a maser oscillator dates as far back as 1959: A. N. Oraevskii, Radiotekh. Elektron. **4**, 718 (1959). More recent studies include M. B. Spencer and W. E. Lamb, Jr., Phys. Rev. A **5**, 884 (1972); W. W. Chow, Opt. Lett. **7**, 417 (1982); IEEE J. Quantum Electron. **QE-19**, 243 (1983).

[6](a) L. A. Lugiato, L. M. Narducci, D. K. Bandy, and C. A. Pennise, Opt. Commun. **46**, 64 (1983); (b) D. K. Bandy, L. M. Narducci, C. A. Pennise, and L. A. Lugiato, in *Coherence and Quantum Optics V,* Proceedings of the Fifth Rochester Conference, 1982, edited by L. Mandel and E. Wolf (Plenum, New York, in press); (c) F. T. Arecchi, G. Lippi, G. Puccioni, and J. Tredicce, *ibid.*

[7](a) G. Benettin, L. Galgani, A. Giorgilli, and J. Strelcyn, Phys. Rev. A **14**, 2338 (1976); (b) Meccanica **15**, 9 (1980); (c) I. Shimada and T. Nagashima, Prog. Theor. Phys. **61**, 1605 (1979).